

# Numerical study of fracture mechanism in ceramic armor under impact load

M.K. Khan, M.A. Iqbal, V. Bratov, N.K. Gupta, N.F. Morozov  
ashraf@rediffmail.com

## Abstract

A numerical investigation has been carried out for studying the fracture mechanics and the ballistic response of ceramic target. The ceramic considered was Alumina 95, the backing plate was Aluminium alloy 2024-T3 and the projectile was made up of Steel 4340. The diameter to length ratio of conical and blunt nosed projectiles has been varied as 0.25, 0.5 and 1.1 keeping the mass constant in order to study the effect of diameter of projectile. The Johnson-Holmquist (JH2) constitutive model has been used for ceramic and the Johnson-Cook (JC) model has been used for the metallic backing material and the projectile. The thickness of target plate and backing plate was 6 mm both, and the size of the plates considered was 150 mm  $\times$  150 mm. A range of velocity has been considered to explore the effect on higher as well as lower velocities. The residual velocities being compared and presented here for different diameters. The ballistic limit velocity (BLV) was also found for different projectile diameter. The BLV was found to be higher with the increase in the projectile diameter. Three dimensional numerical simulation have been performed using ABAQUS/explicit finite element. The simulations were validated with the experimental data.

## 1 Introduction

Ceramic is used as an armor material due to its high compressive strength, hardness and low density. Ceramic possesses low fracture toughness and less tensile strength that cannot be overlooked as these properties are equally important for proper function of armor. Metallic plates or composite layers are used with the ceramic to impart ductility and tensile strength to the protective system. With ceramics as front layer, metals or composites are used as a backing material. Bi-layer armors are found to be efficient in protection as well as being lightweight in comparison to monolithic armors. If ceramic is used with no backing plate or cover, under high impact load it will break instantaneously due to very little toughness it possesses. The function of ceramic layer is to shatter and blunt the projectile, during this process, the ceramic is also fractured but the backing layer keeps the ceramic in its place and absorbs the energy of the projectile by deforming.

The use of bi-layer armor systems, comprising a hard ceramic front face and an

energy absorbing metal backing layer, results in a lighter design compared to monolithic metallic armor providing the same ballistic protection level, against armor-piercing (AP) projectiles. A negligible proportion of the projectile's kinetic energy (0.2 %) dissipates into fracture of the ceramic. The major energy dissipating mechanisms were identified as plastic deformation of both the backing plate (20-40 %) and the penetrator (10-15 %), and the kinetic energy picked up by the ceramic debris (45-70 %) [1990, Woodward].

During high velocity impact a compressive shock wave travels through the thickness of the target, which result in radial cracks in front of the projectile head. A tensile wave came back from the interface and it originates circumferential cracks in the rear face and ceramic conoid is formed. The projectile pushes the comminuted ceramic which is restrained by the backing plate, the backing plate is deformed and bent, it provides space for the comminuted ceramic to move. New fracture conoid with smaller diameter is formed and segregated from the adjoining material and the procedure kept on repeating up to when the diameter of the conoid is closer to the diameter of the deformed projectile. The backing plate reaches its strength and plugs are ejected from the plates having diameter same as the diameter of deformed projectile.

The high velocity impact is a complex process which is affected by many factors. Thickness of the plates, constrained conditions, angle of impact and properties of the materials are few of the factors that affects the fracture mechanics.

Many researchers studied various factors and conditions affecting the ballistic properties in case of bi-layer ceramic-metal armor. Woodward (1990) [1] develops a simple set of models for the perforation of ceramic composite armour, illustrating the relation and effects of various physical properties and impact parameters on the ballistic resistance of the armor. Various aspects like the inertial response of the system components, cone crack formation and projectile erosion and backing deformation were modelled realistically. Woodward (1994) [2] concluded that ballistic performance may be influenced by the nature and thickness of the ceramic, the confining and backing layers and the geometry of the impacting projectile. Zaera and Galvez (1998) [3] presented a new analytical model for simulation of impact problem in case of bi-layer ceramic-metal armor. The model was based on Tate and Alekseevskii's equation for projectile penetration and on the ideas of Woodward's and den Reijer's models for metallic backing and was validated by comparing experimental and analytical results. Some of the experimental works involve Wang and Lu [4]. Based on an existing model, a design criterion has been developed by Wang and Lu (1994), which gives the optimum thickness ratio that gives the best ballistic limit performance of two-component ceramic armour under a given total thickness. The ceramic was used 94 % purity alumina and for backing plate aluminium 6061 T6 and the projectile was NATO 7.62 AP, 0.5 (12.7 mm) calibre. The model used was given by Florence (1969). The model assumes a short cylindrical rod striking normally into the ceramic, and forcing it to break progressively into a cone of fractured material, which distributes all the impact energy to the backing plate over a larger area than the projectile's diameter. The backing plate will deform as a uniform membrane under constant tension. As the energy dissipated in ceramic fracture and projectile erosion is ignored, the failure mechanisms of the backing plate

are simplified significantly. Based on the above assumption, Florence managed to obtain a fairly simple expression for the ballistic limit for two-component armour. To provide a specified level of protection at minimum weight Hetherington (1992) [5] developed an equation for obtaining the optimum thickness ratio. The model was developed under a given aerial density with the total thickness of the armour not being constant. Programme of trials with 7.62AP ammunition against alumina/aluminium combinations confirmed the usefulness of the model. Hetherington observed that for a given areal density, better performance can be obtained with ratios of ceramic to the backing plate as one, or more, and that ratios of less than one can lead to greatly reduced performance. For a normal impact on ceramic target with thin metallic backing plate a model was proposed by Cortes et al. [6] that was based on finite difference Lagrangian formulation. No front confinement was considered there and penetrator considered was made up of steel, and target was constituted of Alumina front plate and aluminium backing plate. The macroscopic material behaviour in the zone of finely pulverized ceramic ahead of the penetrator was modelled by means of a constitutive relation taking into account internal friction and volumetric expansion. When the ceramic is pulverized in front of projectile head, the projectile starts to push it rather than penetration. Lee and Yoo (2001) [7] done experimental and simulation work to find optimum ratio of thicknesses of ceramic and back plate in bi-layer armor as it can also affect the penetration process. Experimental works involve ballistic limit velocity determination of different thickness ratios and the results were used for verification of numerical approach. The armor was constituted of alumina ceramic ( $3380 \text{ kg/m}^3$ ) front plate and 5083 aluminium back plate and the projectile used was made up of steel ( $7850 \text{ kg/m}^3$ ). The Mohr-Coulomb (MC) strength model and linear equation of state (EOS) were used for simulation in AUTODYN hydrocode by using SPH (Smoothed particle hydrodynamics). Using available experimental data Chi et al. (2013) [8] validated numerical simulation model and proposed a semi-analytic ballistic limit velocity model. Using numerical simulations they concluded that for a particular bi-layer armor under same geometric ratios the residual velocity remains same. Serjouei et al. (2015) [9] validated numerical simulation model by using the data of experiments they performed. The numerical simulations then used for validating the model proposed by chi et al. (2012). Numerical simulation was used for finding optimum thickness ratios of ceramic and metal plates. For lower velocities they suggested monolithic metallic armor and for higher velocities ratios of 0.5 and 0.6 was found to be optimum. Venkatesan et al. (2017) [10] studied the behaviour of different aluminum alloys backing plate against ogive nose projectile by using numerical simulation. Venkatesan et al. (2017)[11] compared the ballistic performance of Alumina and Silicon Carbide ceramic using numerical simulation and found Silicon Carbide performance better in a bi-layer armor.

In the present study, numerical simulation model was validated by using experimental data of serjouei et al. (2015). The effect of diameter on residual velocities was studied by comparing the residual velocities for different length to diameter ratios, with mass being constant. Blunt and ogival nose shape has been considered. The ballistic limit velocity was found to be higher in lower length to diameter ratios.

## 2 Numerical Simulation

The ballistic experiments are tedious and also too expensive to perform large number of experiments to gain a full insight of the complex phenomenon. Numerical simulation helps in by giving many detailed observations if proper model and parameters are used. There are many models available, among which Johnson-Holmquist model is widely used for ceramic under high velocity impact, high strain rate and large deformation. The Johnson and Holmquist  $\text{JH}2$  [12] model was used for ceramic and Johnson-Cook model was used for metallic projectile and backing plate. The parameters taken from Serjouei et al. (2015) are presented in table 1 and 2.

### Johnson and Holmquist-2 Model

The normalized equivalent stress is

$$\sigma^* = \sigma_i^* D(\sigma_i^* - \sigma_f^*) \quad (1)$$

Where  $\sigma_i^*$  is the normalized intact equivalent stress, and  $\sigma_f^*$  the normalized fracture stress, and  $D$  is the damage ( $0 \leq D \leq 1.0$ ).

The normalized equivalent stresses ( $\sigma^*, \sigma_i^*, \sigma_f^*$ ) have the general form

$$\sigma^* = \frac{\sigma}{\sigma_{HEL}} \quad (2)$$

Where  $\sigma$  is the actual equivalent stress and  $\sigma_{HEL}$  is the equivalent stress at the HEL. The normalized intact strength is given by

$$\sigma_i^* = A(P^* + T^*)^N (1 + C \ln \dot{\epsilon}^*) \quad (3)$$

and the normalized fracture strength is given by

$$\sigma_f^* = B(P^*)^M (1 + C \ln \dot{\epsilon}^*) \quad (4)$$

The material constants are  $A, B, C, M, N$ , and  $SFMAX$ .

The normalized pressure is

$$P^* = \frac{P}{P_{HEL}} \quad (5)$$

Where,  $P$  is the actual pressure and  $P_{HEL}$  is the pressure at the HEL. The normalized maximum tensile hydrostatic pressure is

$$T^* = \frac{T}{P_{HEL}} \quad (6)$$

Where,  $T$  is the maximum tensile hydrostatic pressure the material can withstand. The dimensionless strain rate is

$$\dot{\epsilon}^* = \frac{\dot{\epsilon}}{\dot{\epsilon}_0} \quad (7)$$

where  $\dot{\epsilon}$  is the actual strain rate and  $\dot{\epsilon}_0 = 1.0 \text{ s}^{-1}$  is the reference strain rate.

The damage for fracture is accumulated in a manner similar to that used in the JH-1 model and the Johnson-Cook fracture model. It is expressed as

$$D = \Sigma \frac{\Delta \epsilon^p}{\Delta \epsilon_f^p} \quad (8)$$

Where,  $\Delta \epsilon^p$  is the plastic strain during a cycle of integration and  $\epsilon_f^p = f(P)$  is the plastic strain to fracture under a constant pressure, P. The specific expression is

$$\epsilon_f^p = D_1(P^* + T^*)^{D_2} \quad (9)$$

Where  $D_1$  and  $D_2$  are constants.

The hydrostatic pressure before fracture begins ( $D = 0$ ) is simply

$$P = K_1\mu + K_2\mu^2 + K_3\mu^3 \quad (10)$$

Where,  $K_1$ ,  $K_2$  and  $K_3$  are constants (  $K_1$  is the bulk modulus); and

$$\mu = \frac{\rho}{\rho_0} - 1 \quad (11)$$

For current density  $\rho$  and initial density  $\rho_0$ . After damage begins to accumulate ( $D > 0$ ), bulking (pressure increase and/or volumetric strain increase) can occur. Now an additional incremental pressure,  $\Delta P$ , is added, such that

$$P = K_1\mu + K_2\mu^2 + K_3\mu^3 + \Delta P \quad (12)$$

### Johnson-Cook Model

The Johnson-Cook (JC) constitutive model describes the strength of engineering alloys at large strains, high strain rates and high temperatures. The flow stress is expressed as an explicit function of strain, strain rate and temperature as follows [13]:

The equivalent stress of the model is defined as

$$\sigma_0 = [A + B(\bar{\epsilon}^{pl})^n][1 + C(\frac{\dot{\bar{\epsilon}}^{pl}}{\dot{\epsilon}_0})][1 - T^m] \quad (13)$$

Where,  $\bar{\epsilon}^{pl}$  is equivalent plastic strain, A, B, n and m are material parameters measured at or below the transition temperature,  $T_0$ . The non-dimensional temperature  $\hat{T}$  is defined as:

$$\hat{T} = \begin{cases} 0, & \text{for } T < T_0 \\ \frac{T-T_0}{T_{melt}-T_0}, & \text{for } T_0 \leq T \leq T_{melt} \\ 1, & \text{for } T > T_{melt} \end{cases}$$

Where, T is the current temperature,  $T_{melt}$  is the melting point temperature and  $T_0$  is the transition temperature defined as the one at or below which there is no temperature dependence on the expression of the yield stress.

When  $T > T_{melt}$  the material melts down and behaves like fluid and hence does not

Table 3: Parameters for Alumina 95%

S.No.	Parameter	Values
1.	Density( $\text{Kg}/\text{m}^3$ )	3741
2.	EOS	Polynomial
3.	Bulk Modulus $K_1$ (GPa)	184.56
4.	Pressure Constant, $K_2$ (GPa)	185.87
5.	Pressure Constant, $K_3$ (GPa)	157.54
6.	Strength Model	JH-2
7.	Shear Modulus G (GPa)	120.34
8.	Hugoniot,elastic limit (HEL) (GPa)	6
9.	Intact strength constant, A	0.889
10.	Intact strength exponent, N	0.764
11.	Strain rate constant, C	0.0045
12.	Fracture strength constant, B	0.29
13.	Fracture strength exponent, M	0.53
14.	Normalized maximum fractured strength	1
15.	Failure model	JH-2
16.	Normalized hydrostatic tensile limit, $T^*$ (GPa)	-0.3
17.	Damage constant, d1	0.005
18.	Damage constant, d2	1
19.	Bulking factor, $\beta$	1

offer shear resistance.

The projectile of nominal diameter 7.56 mm and a nominal length of 30.54 mm was used. The target was a bi-layer with a front plate of size 100 mm  $\times$  100 mm and back layer size was 160 mm  $\times$  160 mm. The materials of projectile, front layer and back layer of target were hardened steel 4340, Alumina 95% and Aluminium alloy 2024-T3 respectively.

Three dimensional finite element model of the bi-layer armor and projectile was made in ABAQUS/CAE. The projectile and target plates both were modelled as deformable bodies with Lagrangian elements. The four peripheral boundaries of the target was restrained against all degree of freedom. The size of the mesh for target plates was kept constant in all cases i.e. 0.6 mm in the inner part of 60 mm and increasing gradually towards the peripheral boundaries. The mesh of size 0.65 mm was kept for projectile. Eight node brick element (C3D8R) were considered for plates. The numerical simulation was found to be in good agreement with the experiments and found to be suitable for predicting the failure behaviour of concerned bi-layer ceramic armor.

Table 4: Parameters for Aluminium and Steel.

S. No.	Parameters	Al-2024-T3	Steel 4340
1.	Density	2785	7770
2.	EOS	Shock	Linear
3.	Bulk Modulus, $K_1$ (GPa)		159
4.	Gruneisen constant	2	
5.	Parameter C1 (m/s)	5328	
6.	Parameter S1	1.338	
7.	Specific heat, Cr (J/kg.K)	874.9	477
8.	Strength Model	JC	JC
9.	Shear Modulus, G (GPa)	26.92	77
10.	Static yield strength, A (GPa)	0.167	0.950
11.	Strain hardening constant, B (GPa)	0.596	0.725
12.	Strain hardening exponent, n	0.551	0.375
13.	Strain rate constant	0.001	0.015
14.	Thermal softening exponent, m	0.859	0.625
15.	Melting temperature, (K)	893	1793
16.	Reference strain rate	1	1
17.	Failure model	JC	JC
18.	Damage constant, d1	0.112	-0.8
19.	Damage constant, d2	0.123	2.1
20.	Damage constant, d3	1.5	-0.5
21.	Damage constant, d4	0.007	0.002
22.	Damage constant, d5	0	0.61

### 3 Results and Discussion

#### 3.1 Validation

The experimental data of Serjouei et al. (2015) was used. The size of the ceramic front layer and metallic backplate target plates was kept 150 mm  $\times$  150 mm. The thickness of the plates was considered to be 6 mm. During the experiments, an obliquity was experienced, the impact was not perfectly normal to the target surface. That inherited yaw angle was considered in the numerical simulation model also as shown in fig. 1.

A comparison was made in residual velocity and residual length of the projectile. After perforation of the target plates, the hole created in the plates was measured at the rear side of the backing plate in two mutually perpendicular directions namely a1 and a2. The errors in residual velocity, residual length, a1 and a2 was found to be very less, and reported in table 3. The numerical simulation was found to be in good agreement with the experiments and found to be suitable for predicting the failure behaviour of concerned bi-layer ceramic armor.

Table 5: My caption

Parameter	Experiment	Simulation	%Error
Residual Length	23.4 mm	25.2 mm	7.6
Residual Velocity	351 m/s	355 m/s	1.1
a1	14 mm	12.9	7.8
a2	16 mm	15.1	5.6

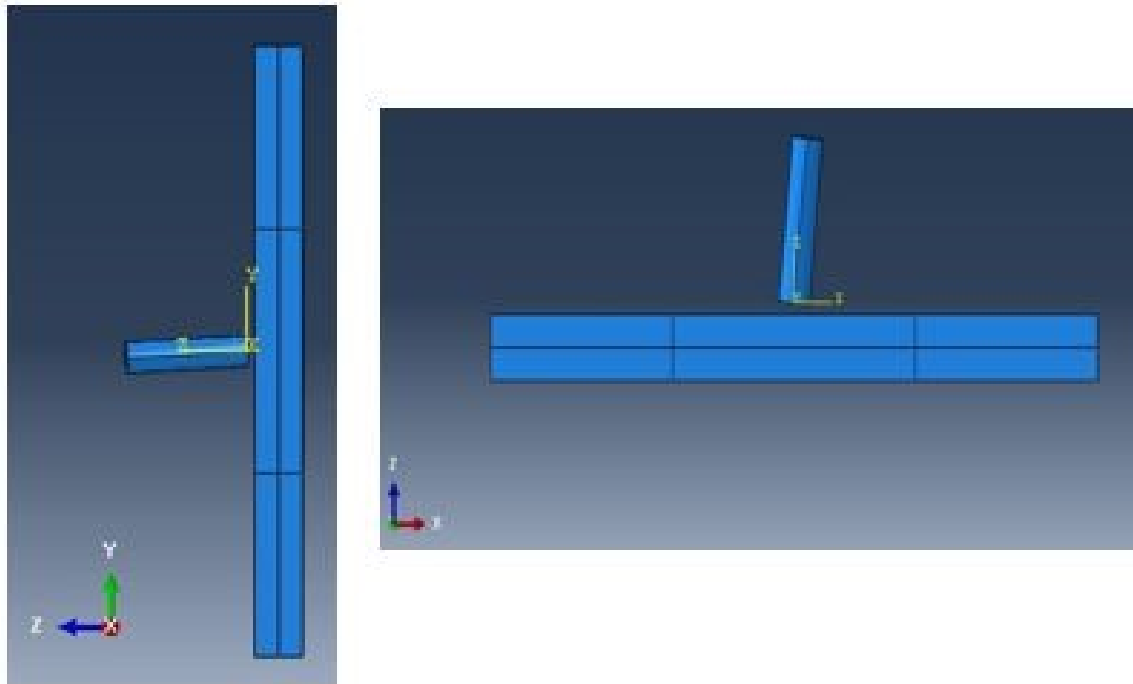


Figure 1: Angel of yaw.

### 3.2 Effect of diameter variation

The nominal diameter of the projectile in study of Serjouei et al. (2015) was 7.56 mm with a nominal length of 30.54 mm. The ballistic limit was worked out by using numerical simulation and was found to be 435 m/s. The diameter of the projectile here taken as 10 mm and 12.5 mm. The length of projectile was changed accordingly as 17.45 mm and 11.17 mm to maintain the mass of the projectile to be constant. In both the cases of blunt head and ogival nose head the residual velocity was found to be increasing with decreasing diameter to length ratios. The comparison for blunt nose head projectile have been shown in fig. 3.

Table 6: BLV for different D/L ratios.

S.No.	D/L Ratio	BLV (m/s)
1.	0.25	435
2.	0.5	565
3.	1.1	615



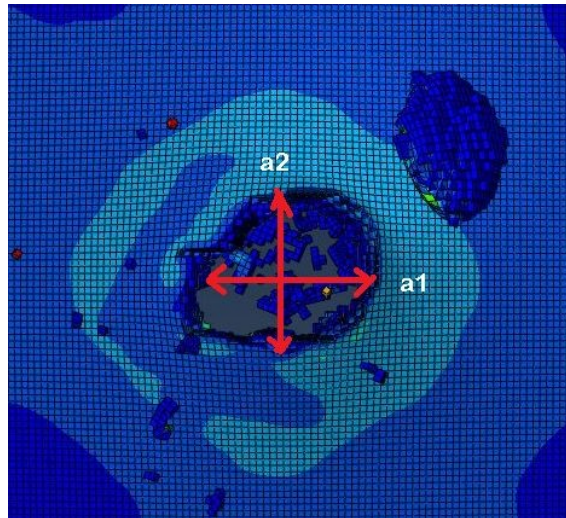


Figure 2: Damage in terms of size of the hole at rear face of baking plate.

The comparison of ogival nose head projectile have been shown in fig. 4. The residual velocity was found to decreasing with the increase in the diameter of the projectile. The phenomenon can be attributed to the more interaction of the deformed projectile with the comminuted ceramic. The ballistic limit velocity was found for the blunt projectiles. It was found to be increased with the increased diameter to length ratios for all cases. The ballistic velocities are mentioned in table 4.

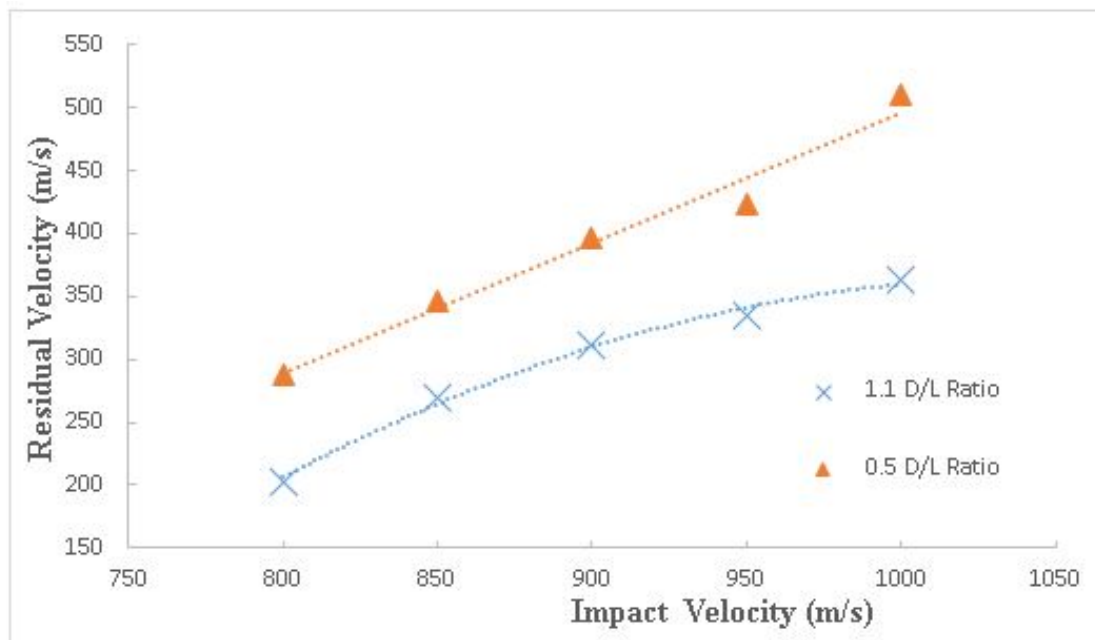


Figure 3: Residual velocity for blunt projectile.

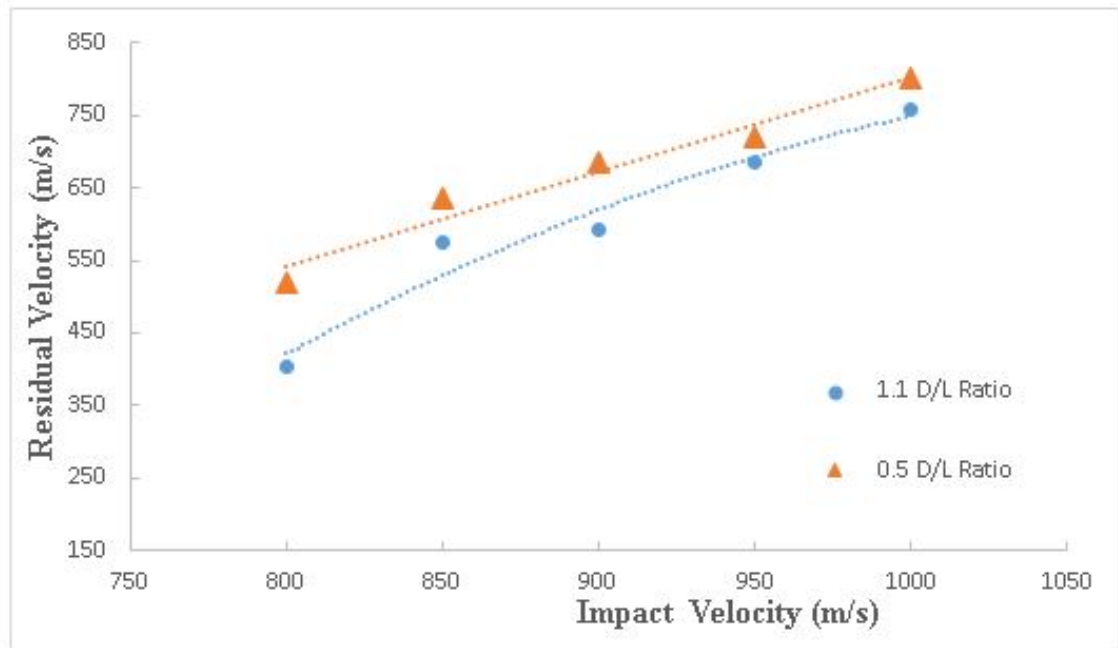


Figure 4: Residual velocity for Ogive nose projectile.

## 4 Conclusions

Numerical simulation was validated by using experimental data available in open literature. Effect of diameter to length ratios was studied by using 3D numerical simulation. The residual velocities was found to be decreasing with the increase in diameter of the projectile. The ballistic limit velocity was increased with the increased diameter. This can be attributed to the increased interaction between comminuted ceramic and projectile.

## Acknowledgements

*Authors gratefully acknowledge the financial support provided by Department of Science and Technology through grant no. INT/RUS/RFBR/P-232 under DST-RFBR scheme for carrying out this research work.*

## References

- [1] Woodward, Raymond LA simple one-dimensional approach to modelling ceramic composite armour defeat, *International Journal of Impact Engineering*, **9**, 1990, 455–474.
- [2] Woodward, RL and Gooch Jr, WA and O'donnell, RG and Perciballi, WJ and Baxter, BJ and Pattie, SD, A study of fragmentation in the ballistic impact of ceramics, *International Journal of Impact Engineering*, **15**, 1994, 605–618.

- 
- [3] Zaera, R and Sánchez-Gálvez, Vicente, Analytical modelling of normal and oblique ballistic impact on ceramic/metal lightweight armours, *International Journal of Impact Engineering*, **21**, 1998, 133–148.
- [4] Wang, B and Lu, G and Lim, MK, Experimental and numerical analysis of the response of aluminium oxide tiles to impact loading, *Journal of materials processing technology*, **51**, 1995, 321–345.
- [5] Hetherington, JG, The optimization of two component composite armours, *International Journal of Impact Engineering*, **12**, 1992, 409–414.
- [6] Cortes, R and Navarro, C and Martinez, MA and Rodriguez, J and Sanchez-Galvez, V, Numerical modelling of normal impact on ceramic composite armours, *International Journal of Impact Engineering*, **12**, 1992, 639–650.
- [7] Lee, M and Yoo, YH, Analysis of ceramic/metal armour systems, *International Journal of Impact Engineering*, **25**, 2001, 819–829.
- [8] Chi, Runqiang and Serjouei, Ahmad and Sridhar, Idapalapati and Tan, Geoffrey EB, Ballistic impact on bi-layer alumina/aluminium armor: A semi-analytical approach, *International Journal of Impact Engineering*, **52**, 2013, 37–46.
- [9] Serjouei, Ahmad and Chi, Runqiang and Zhang, Zhiyuan and Sridhar, Idapalapati, Experimental validation of BLV model on bi-layer ceramic-metal armor, *International Journal of Impact Engineering*, **77**, 2015, 30–41.
- [10] Venkatesan, J and Iqbal, MA and Gupta, NK and Bratov, V and Kazarinov, N and Morozov, F, Ballistic Characteristics of Bi-layered Armour with Various Aluminium Backing against Ogive Nose Projectile, *Procedia Structural Integrity*, **6**, 2017, 40–47.
- [11] Venkatesan, J and Iqbal, MA and Madhu, V, Ballistic performance of bilayer alumina/aluminium and silicon carbide/aluminium armours, *Procedia Engineering*, **173**, 2017, 671–678.
- [12] Johnson, Gordon R and Holmquist, Tim J, An improved computational constitutive model for brittle materials, *AIP Conference Proceedings*, **309**, 1994, 981–984.
- [13] Johnson, Gordon R, Cook W.H., A constitutive model and data for metals subjected to large strains, high strain rates and high temperatures, *Proceedings of the 7th International Symposium on Ballistics*, 1983.

M. A. Iqbal, Department of Civil Engineering, IIT Roorkee, Roorkee-247667, India